

## **Rib strain fields corridors in side and oblique impact based on PMHS tests**

Pascal Baudrit and Tiphaine Leport  
CEESAR

*This paper has not been screened for accuracy nor refereed by any body of scientific peers  
and should not be referenced in the open literature.*

### **ABSTRACT**

*This paper presents the results of a study performed in the framework of the European THOMO project. The objective is to define corridors of rib strain fields measured on human ribs in side and oblique impacts. These corridors could define validation targets for models or dummies. In 2008, Trosseille et al has shown the interest to measure rib strain on post-mortem human subjects, in order to discriminate several loading conditions (hub, airbag) in side, oblique and frontal impact. Moreover, the rib strains were strongly linked to the rib fracture location. In order to build corridors of strain fields, a set of twelve post-mortem human subject dynamic tests were performed in side and oblique impact, in order to complete existing tests. The ribcage was instrumented with more than 100 strain gauges on the rib, cartilage and sternum. The paper presents the methodology and the test results, regarding the injuries and measurements. The results of the analysis of rib strain gauges are shown. Rib strain fields corridors are given in side and oblique impacts, for impactor and airbag tests. Several perspectives are given using these data for the development of finite-element models, and specifically for the development of the Thorax of the Global Human Body Model.*

### **INTRODUCTION**

**H**uman body models are more and more used in automotive field as tools for the assessment of real safety. For the thorax, validation targets exist for the global mechanical behavior. Most of them regard force-deflection corridors in frontal, side, oblique impacts (Kroell et al, 1971 and 1974, Shaw et al, 2006). For the hard tissues, and specifically for the ribs or ribcage, tests on isolated parts and samples were

performed in the past and used as validation targets for the cortical bone material (Charpail et al, 2005, Kemper et al, 2005), and sub-structures (Kent et al, 2004). For the validation of rib fracture mechanisms on complete thorax with loadings close to those encountered in automotive crash, few data exist. In 2008, Trosseille et al has shown a promising methodology, using strain gauges glued on the ribs of post-mortem human subjects (PMHS) and a specific signal analysis has been developed. Strain profiles can be drawn and it has been shown that the rib fracture location is in very good accordance with the maximum absolute strain location. Then, the strain is considered as a good candidate for a “micro-criterion”. Using this methodology, some of existing tests have been duplicated in the same conditions, in order to build corridors of strain profiles in different loadings and direction of forces, in side and oblique impact. The paper presents the methodology and results, with a focus on the 5<sup>th</sup> rib of the impacted side.

## METHODS

The method used for this study has been described by Trosseille et al (2008). The main parts are reminded here-after. A test protocol on post-mortem human subjects has been developed for acquiring rib strains by means of strain gauges, up to 96 glued on the ribcage. Four series of dynamic tests were performed on the thorax:

- deployment of an unfolded airbag at different distances in pure side impact.
- deployment of an unfolded airbag at different distances in oblique forward impact.
- 23.4 kg rigid impactor tests at 4.3 and 6.7 m/s in pure side impact.
- 23.4 kg rigid impactor tests at 4.3 and 6.7 m/s in oblique forward impact.

A set of fourteen tests were published by Trosseille et al in 2008 and 2009. Eight tests are performed for the present study, in the frame of the European THOMO project (7<sup>th</sup> Framework Program).

### Subject preparation

The PMHS were obtained through the Body Donation to Science at the Saints Pères University of Medicine in Paris Vth after approval of the experimental procedures by the ethical and scientific committee of the university. The PMHS were tested for Cytomegalovirus (CMV), Human T cell Leukemia/lymphoma Virus (HTLV), Hepatitis C Virus (HCV), Hepatitis B Virus (HBV) and Human Immunodeficiency Virus (HIV), and a medical survey was documented. PMHS suspected of bone fragility (long bed stay, bone cancer, metastasis, etc.) were excluded. They were chosen to be as close as possible to a 50<sup>th</sup> percentile male. The PMHS were frozen and then thawed at room temperature during 48 hours before preparation. Their main characteristics are reported in Table 1.

**Table 1: main characteristics of the post-mortem human subjects used for the study**

#	Sexe (M/F)	Age (years)	Weight (kg)	Stature (m)
568	M	51	54	1.75
569	F	53	54	1.63
570	M	66	87	1.86
571	M	79	75	1.67
572	M	68	68	1.74
573	M	68	75	1.72
574	M	76	80	1.67
575	M	72	59	1.56
576	M	73	80	1.76
577	M	76	66	1.62
579	M	87	55	1.59
584	M	82	59	1.61
585	M	89	64	1.68
586	M	74	77	1.76
587	M	82	78	1.80
588	M	88	69	1.67
605	M	73	61	1.71
606	M	87	71	1.71
612	M	82	62	1.62
613	F	65	73	1.60
614	M	80	56.5	1.78
616	M	55	63	1.75
619	M	83	73.5	1.70
620	M	79	63.5	1.67

In order to get realistic pulmonary volumes, the PMHS lungs were inflated once with approximately 2.5 liters of air through a tracheotomy tube which was held closed during the test.

Just prior to the test, the arterial system were pressurized at physiological conditions with a liquid composed of alcohol and India ink. In addition, in order to obtain a more realistic mechanical behavior of the liver which is a highly perfused organ, the inferior vena cava and the portal vein were filled with an isotonic solution (9‰ NaCl) by means of a drip directly connected to these veins.

### **Test setups**

*Impactor tests.* The PMHS thoraces were impacted by a 23.4 kg impactor. The impactor interface was a flat, 152 mm disc as described by Viano (1989). The impactor, propelled by bungees at mean velocities of 4.3 m/s and 6.7 m/s, was guided during the impact. The surrogates were seated on a horizontal low friction rigid plate. The thighs were lying on the low friction plate, the knees were flexed and the feet were lying on footrest.

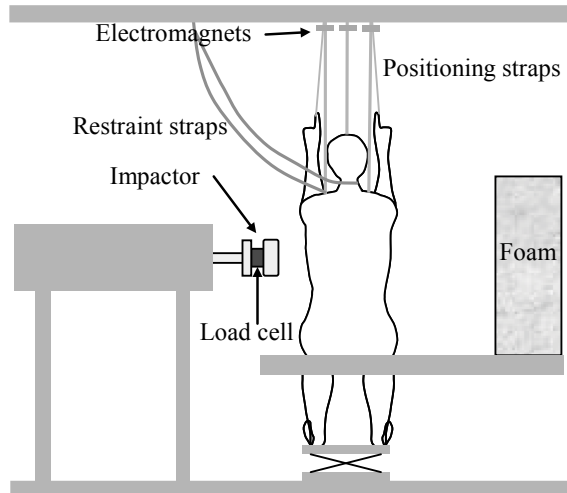


**Figure 1: impactor test set-up (pure side impact position)**

*Airbag tests.* The post mortem human subject was fixed onto a rigid seat and was placed in front of an unfolded airbag (Figure 2). The airbag module was fixed on a rigid steel plate (700 x 400 mm) named “airbag plate”. The driver airbag module described by Petit et al. (2003) and by Lebarbé et al. (2005) was used. The entire cover of the module was removed and the fabric was totally unfolded out of the module in order to eliminate the “punch out” effect. Prior to the test, the residual air volume inside the airbag was removed. The size of the bag was reduced (500 mm in diameter) to be adapted to the lateral thorax dimensions.

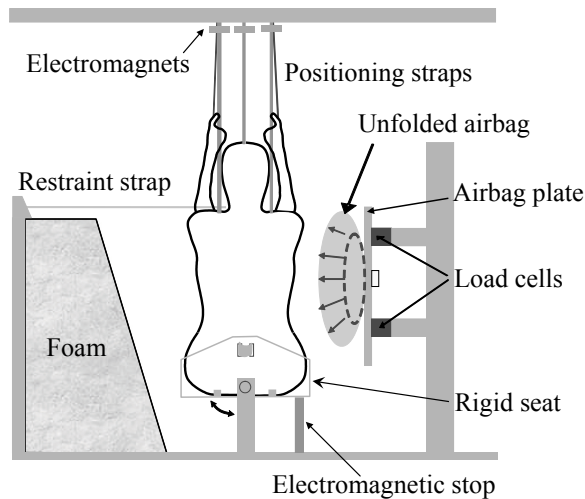


**Figure 2: unfolded airbag test set-up (pure side impact position)**

To fix rigidly the specimen onto the rigid seat, the legs were amputated and each femur was secured to the front of the rigid seat through a shaft screwed into their medullary canal. The pelvis was attached to the rigid seat using a strap wrapped around the 5th lumbar vertebra, and two cables passing through each obturator foramen. The femur anchorages pressed the sacrum backwards against the rigid seat. The only degree of freedom of the pelvis fixation plate was the rotation around the horizontal axis parallel to the airbag plate.

*Supporting system.* The surrogates were held in initial position using straps attached on both clavicles close to the sterno-clavicular joint and on the top of the head. The straps were attached to the frame of the test rig using electromagnets. They were released at the firing time of the airbag or at the impact time.

A soft foam pad was placed at the opposite side of the impact in order to stop the motion of the specimen at the end of the test.

## Positioning procedure

Depending on the configuration, the origin of the laboratory coordinate system was either the center of the impactor or the center of the airbag module.

For the impactor tests, the PMHS was seated on the horizontal rigid plate. For the airbag tests, the PMHS was installed in the rigid seat on the test setup. Once the PMHS was placed on the test setup, the positioning procedure was as following:

- The clavicle straps' lengths and anchorage positions were adjusted to straighten and to position the spine. The spine was set vertical. The initial tension forces recorded in the strap were approximately 150 N for the clavicles and 50 N for the head.

- The lungs were inflated.

- The PMHS position was adjusted according to the configuration. The reference ribs were the 5<sup>th</sup> and the 6<sup>th</sup> for respectively the airbag and impactor tests.

- For the pure lateral tests, the PMHS was positioned such that the middle point of the reference rib (the point of the reference rib at equal distance between the sternum and the spine) was at  $X=0$  and  $Z=0$ .

- For the oblique tests, the entire subject was rotated  $60^\circ$  around a vertical axis from the frontal position. The PMHS was positioned such that the middle point of the reference rib was at  $Z=0$ , and that the half-width of the thorax at the level of  $Z=0$  was at  $X=0$ .

- For the airbag tests, the shortest distance between the airbag plate and the thorax was adjusted according to the test matrix.

- For the impactor tests, lateral and oblique airbag tests, the upper arms were set horizontal (parallel to the airbag plate for airbag tests); the forearms were vertical.

A 3D measuring arm (Romer type 100) was used to digitize the targets and the bone landmarks during the specimen positioning.

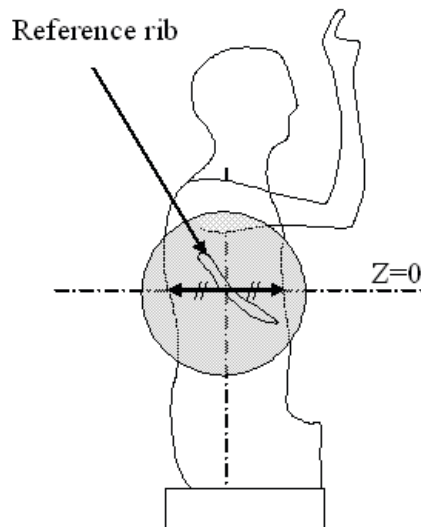


Figure 3: position along the Z-axis for the 90° and 60° tests

## Instrumentation

*Forces.* Four load cells were mounted between the airbag plate and a rigid fixed frame to measure the forces applied onto the thorax. A load cell and an accelerometer were fixed behind the impacting surface of the impactor. The impactor force applied to the surrogate was compensated for inertia.

*Accelerometers.* Triaxial accelerometers were fixed respectively onto the T1, T4, T12 vertebrae. Triaxial accelerometers were fixed onto the sternum (upper and lower parts).

*Strain gauges.* The PMHS rib cages were instrumented with strain gauges glued on the external rib part, according to a protocol developed by Potier (2010). Care was taken to keep the muscles intact and to align the measurement axis of the strain gauges with the long axis of the rib. Then, the skin was sutured. A positive signal indicates tension, and a negative signal indicates tension.

The location of the strain gauges was defined by the wrap-around distance (WAD) measured along the fifth rib with a tape. It was given with respect to the costo-transverse joint (CTJ) (Figure 6). In the paper, the curvilinear abscissa ( $s$ ) is defined by the following formula (Equation 1):

**Equation 1:**

$$s = \pm \frac{wad(strain\_gauge)}{wad(CCJ)} * 100$$

The sign of  $s$  is negative for the left ribs and positive for the right ribs.  $s=0\%$  at the costo-transverse joint (CTJ) and  $s=100\%$  at the costochondral joint (CCJ).

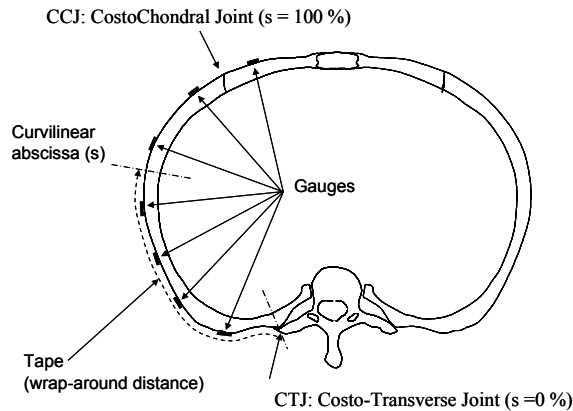


**Figure 4:** definition of the curvilinear abscissa

## Test matrix

The test experiments are described in Table 2. Eight of the twenty-four experiments have been performed in the frame of the European THOMO project; the other experiments come from Trosseille et al (2008, 2009).

**Table 2: test matrix for the four configurations (in blue color, tests performed in the THOMO project)**

<b>PMHS</b>	<b>TEST CONDITIONS</b>		
#	Loading	Angle	Speed (m/s) or distance (mm)
572	Airbag	60	114 mm
571	Airbag	60	123 mm
573	Airbag	60	178 mm
575	Airbag	60	200 mm
576	Airbag	60	208 mm
574	Airbag	60	211 mm
569	Airbag	90	98 mm
584	Airbag	90	112 mm
585	Airbag	90	123 mm
568	Airbag	90	118 mm
570	Airbag	90	137 mm
588	Airbag	90	140 mm
577	Airbag	90	189 mm
579	Airbag	90	211 mm
587	Impactor	60	4.2 m/s
606	Impactor	60	4.2 m/s
613	Impactor	60	4.2 m/s
614	Impactor	60	6.5 m/s
620	Impactor	60	6.5 m/s
586	Impactor	90	4.4 m/s
605	Impactor	90	4.3 m/s
612	Impactor	90	4.3 m/s
616	Impactor	90	6.5 m/s
619	Impactor	90	6.5 m/s

### Post-test procedure

An in-depth necropsy, focused on the thorax, was performed after the tests. The rib fractures were classified using four categories:

- complete with displacement (D)
- complete without displacement (ND)
- partial with rupture of the external cortical bone (PE)
- partial with rupture of the internal cortical bone (PI)

For the clinical AIS, only the complete fractures with displacement have been counted, as they are the only ones that would be detected by standard thoracic X-ray. The clinical AIS can therefore be compared to the AIS in the crash investigation studies. For the autopsy AIS, all the fractures have been counted.

The location of the rib fractures was measured using the wrap-around distance from the costo-transverse joint.

For a more understandable visual display of the rib fracture location, the rib fractures are positioned on a geometrical rib model from Song et al (2009). On the PMHS and the geometrical rib model, the position of rib fracture, in percentage of rib length, are identical. An example is given in Figure 5. It represents an upper view of the thorax with the location of rib fractures.

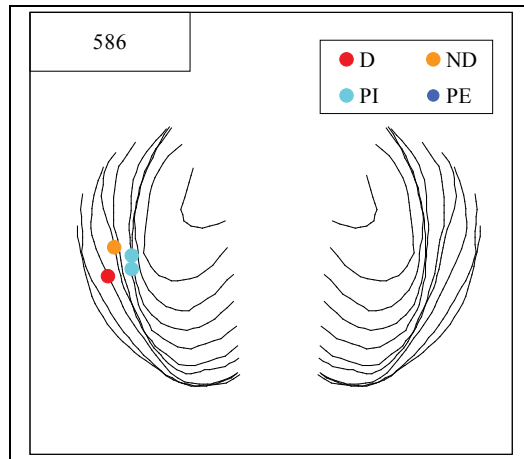


Figure 5: example of visualization of the rib fracture location

### Signal processing

*Filtering.* The forces were filtered CFC180, the spinal and impactor accelerations CFC180, the strains CFC1000 and the strain rates CFC600.

*High speed video.* The tests were filmed using three high-speed cameras at 1000 to 4000 frames-per-second (fps). The views consisted of a frontal and rear global views and a zoom view centered on the thorax. The views were perpendicular to the airbag plate, and parallel to the impactor displacement axis.

### Data analysis

*Strain profiles.* The strain profile on the 5<sup>th</sup> rib on the impacted side (strain as a function of the curvilinear abscissa) can be drawn, as illustrated in Figure 6 at a given time. CTP and CCJ stand respectively for costo-transverse process and costo-chondral joint.

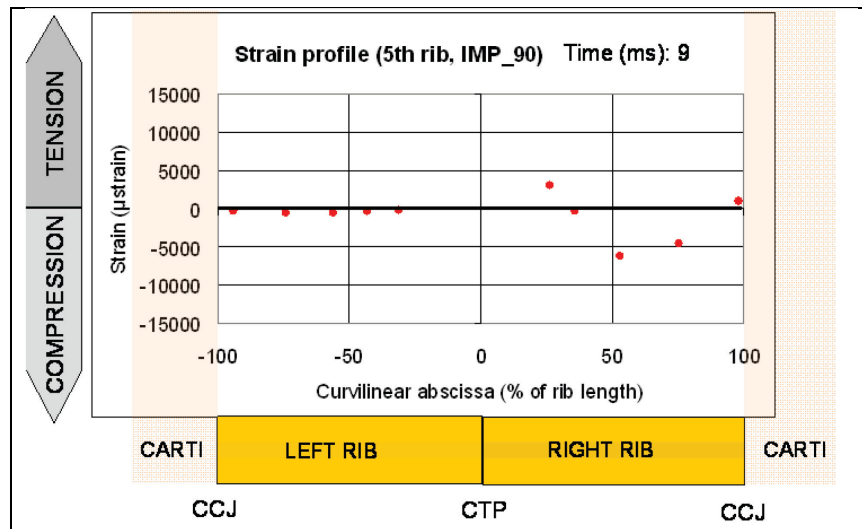


Figure 6: example of strain profile



*Normalized strain profiles.* In order to allow the comparison of different tests, the strains were normalized. For that purpose, the methodology used by Trosseille et al (2008) was modified in order to take into account only the strains measured on the impacted side of the 5<sup>th</sup> rib.

An effective strain,  $\epsilon_{RMS}$  (Root Mean Square) was calculated for each rib (Equation 2). Then, each strain of the rib was divided by the effective strain to obtain a normalized strain  $\epsilon_N(s, t)$  (Equation 3).

$$\text{Equation 2: } \epsilon_{RMS}(t) = \sqrt{\frac{1}{(s_1 - s_n)} \left( \int_{s_n}^{s_1} (\epsilon(s, t))^2 ds \right)}$$

$$\text{Equation 3: } \epsilon_N(s, t) = \frac{\epsilon(s, t)}{\epsilon_{RMS}(t)}$$

*Average normalized strains.* In order to assess the stability of the strain profiles over the time, the average and standard deviation of the normalized strains are calculated. The more important the standard deviation is, the less stable the strain profile is. For non fractured ribs, the window time corresponds to the 10 and 100 % of the normalized strain maximum. For fractured ribs, the window time corresponds to the 10 and 99 % of the normalized strain magnitude at time of rib fracture.

*Corridors.* For each of the four test configurations, a corridor has been built, using the average normalized strains. Because it is impossible to experimentally insure the same curvilinear abscissa of the strain gauges for all the PMHS, the average normalized strains were fitted with a polynomial of (n-1) degrees for n strain gauges for resampling. Then, the average curve and its standard deviation can be calculated for each configuration.

## RESULTS

### General parameters.

*Forces.* For the airbag tests in pure side impact, the mean force applied onto the PMHS was  $4.07 \pm 1.21$  kN. In oblique airbag impact, the mean force was  $3.77 \pm 1.80$  kN. In impactor tests, in pure and oblique side impacts, the mean forces were respectively  $2.66 \pm 0.94$  and  $2.15 \pm 0.50$  kN.

*Thorax injuries.* The table 3 displays the different injuries which have been observed during the necropsies. For the hard tissues, the main injuries regard the rib fractures, with an amount of 196 (including 6 on the far side), whatever the type is. Three sternum fractures were observed in airbag tests, and six fractures of the transverse process. For the soft tissues, pleural hematoma and/or lacerations were found on seven tests in front of the rib fractures.

**Table 3: list of the different injuries observed during the necropsy of the twenty-four tests**

Thoracic part	Injuries (taken into account for the AIS calculation)
Ribs	196 fractures (including 6 on the opposite side)
Sternum	3 fractures (airbag tests)
Vertebra	6 fractures of the transverse process
Soft tissues	Pleural hematoma and/or lacerations in front of the rib fractures (7 PMHS)

**Rib fracture location.**

*Rib fracture locations.* The figures 7, 8, 9 and 10 show the location of rib fractures per configuration. The results show that the position of rib fractures are not so scattered that one could expect. Typical sites of rib fractures can be found, whose position depends on the impact direction. One site of rib fractures is in front of the impactor and or the airbag. A second site of rib fractures, when it exists, is found very close to the costo-vertebral joint in pure side impact, and more anterior in oblique impact tests.

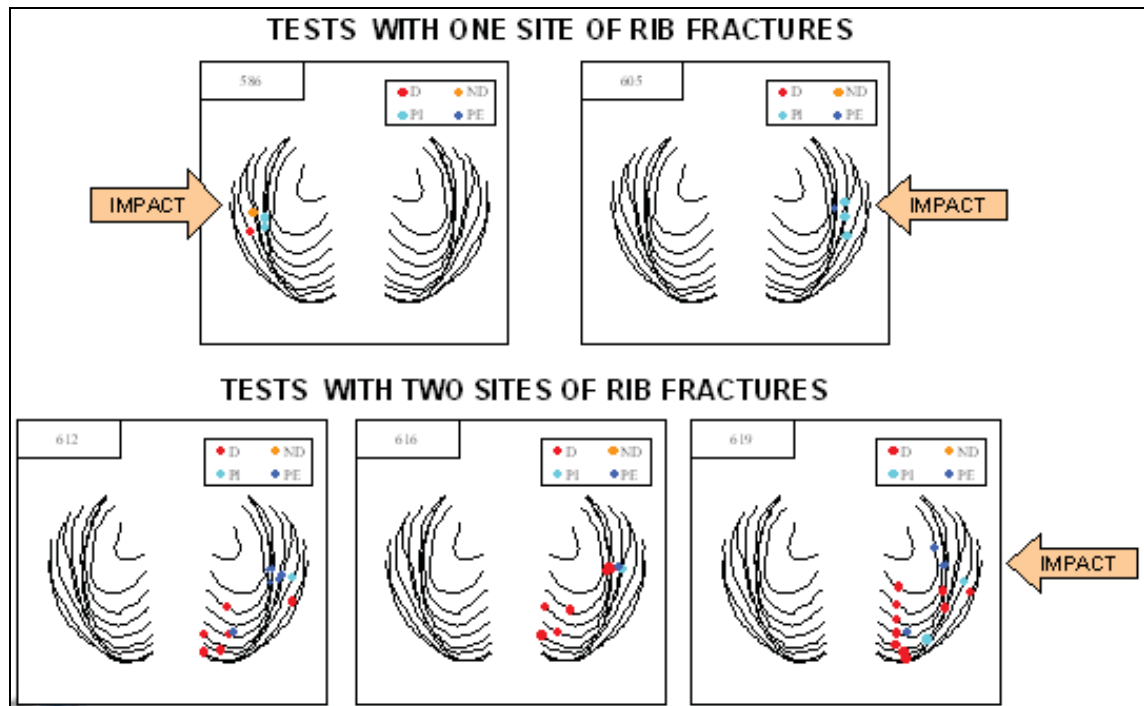


**Figure 7: rib fracture location for impactor tests at 90 degrees**

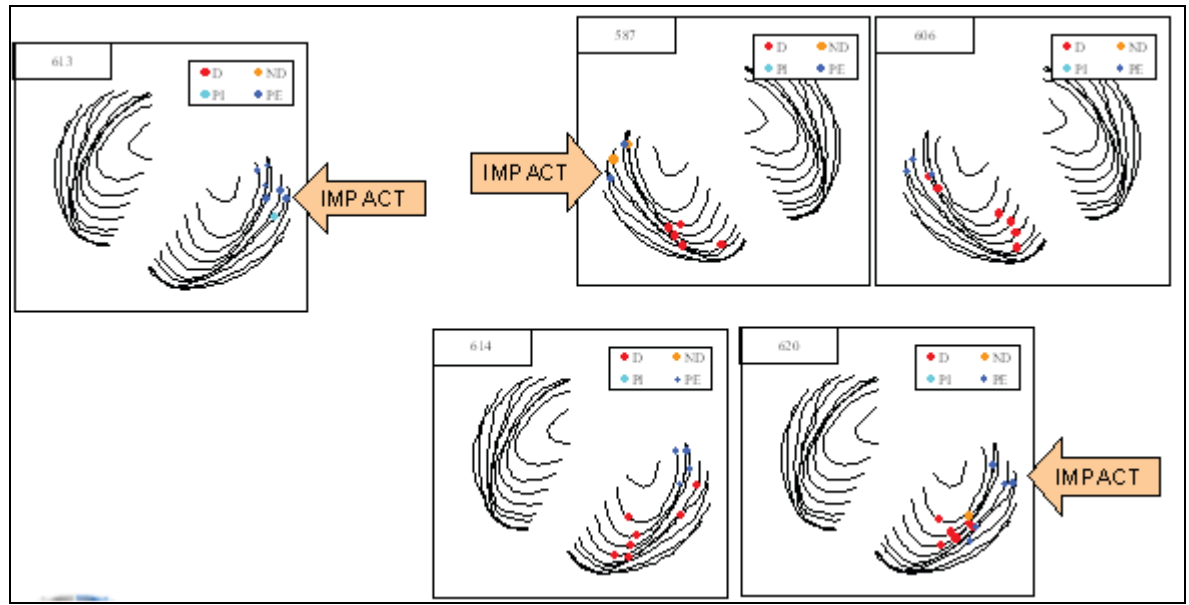


Figure 8: rib fracture location for impactor tests at 60 degrees

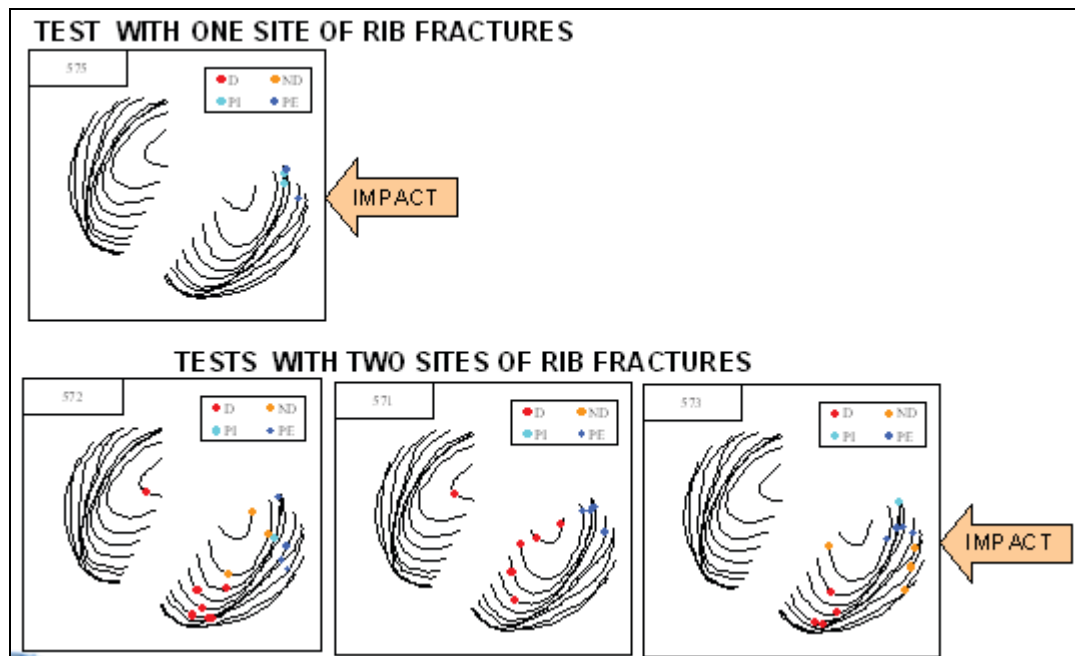


Figure 9: rib fracture location for airbag tests at 60 degrees

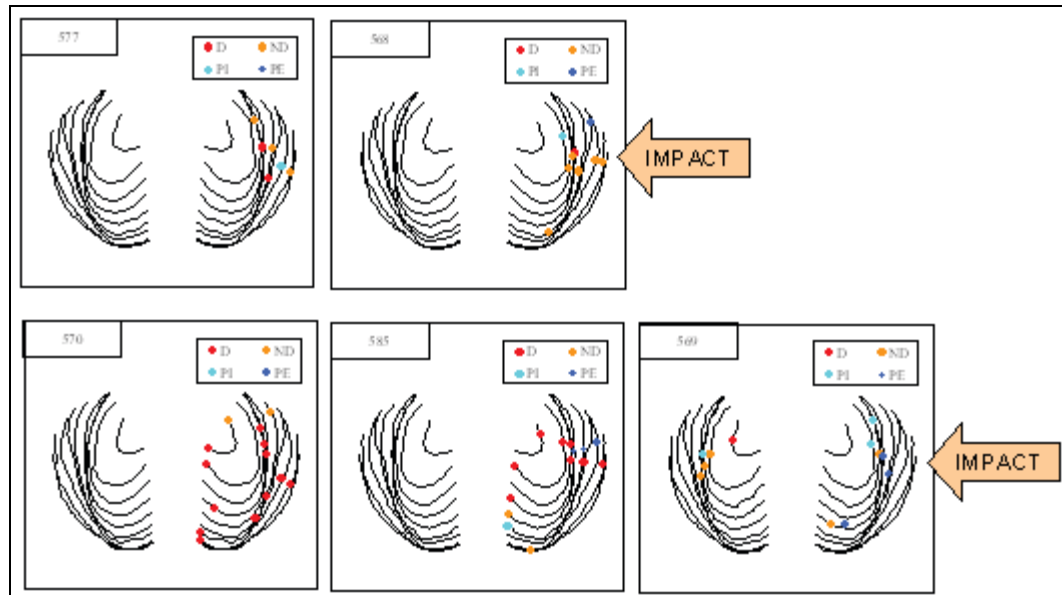


Figure 10: rib fracture location for airbag tests at 90 degrees

## Strain profiles

*Strain profiles.* Figure 11 displays the different mean normalized strain profiles per configuration. They exhibit typical strain patterns, with compression or tension depending on the curvilinear abscissa. In front of the impactor, or in front of the airbag, the strains of the external part of the rib are always negative. For the airbag tests at 90 degrees, the strain minimum is located at 60 % of the rib length. Between 25 % and 35 % of the rib length, the strain is null, and below 25 % of the rib length, the strain is always positive. Between 80 and 95 % of the rib length, the strain is null. For the airbag tests at 60 degrees, the strain is negative above 40 % of the rib length, with a strain minimum located at 80 % of the rib length. Below 40 % of the rib length, the strain is always negative.

For the pure impactor tests, between 30 and 90 % of the rib length, the strain is negative, and positive everywhere else. The strain minimum is between 50 and 70 %. For the impactor tests at 60 degrees, the strain minimum is located close to 80 % of the rib length. Above 60 %, the strain is negative. One test exhibits a strain pattern very different from the others and will be considered as an outlier. It will be removed of the sample for the building of the corridor.

The most violent tests are shown in red for the different configurations. The results of these tests do not show significant differences in comparison with the other tests for all the configurations.

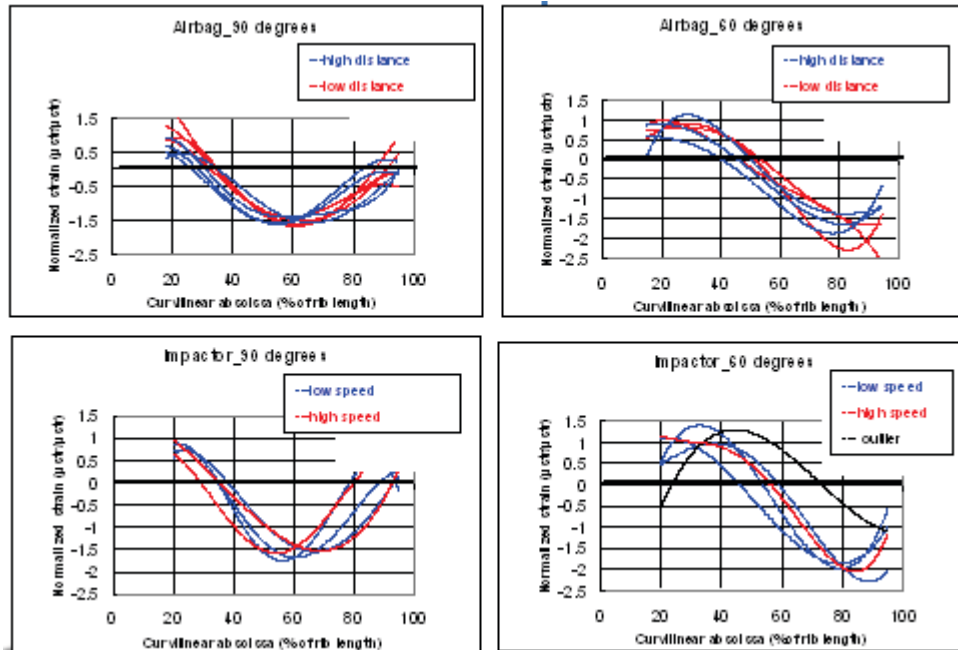


Figure 11: strain profiles on the 5<sup>th</sup> rib on the impact side in four different configurations

Figure 12 shows the corridors obtained for the four configurations. In red, the average curve is shown, and in blue, the mean curves plus and minus one standard deviation are superimposed. The rectangles correspond to the location of rib fractures observed in the tests. The position of rib fractures is in good accordance with the position of the strain extremum.

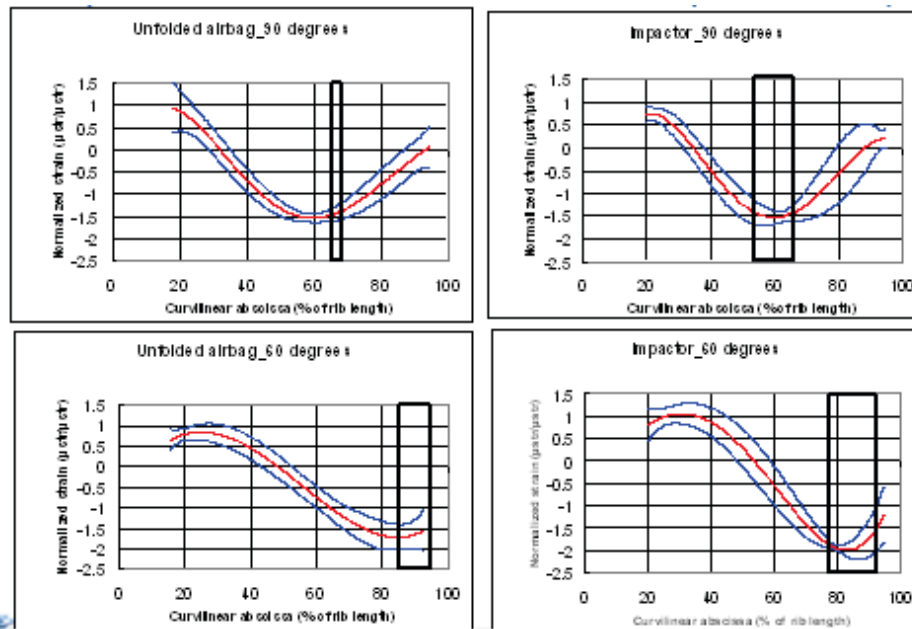


Figure 12: strain profile corridors in side and oblique impact for impactor and airbag tests (mean curves  $\pm$  SD, rectangles show the rib fracture location)

## DISCUSSION

### Effect of angle.

On Figure 13, the mean curves of strain profiles at 60 and 90 degrees, for the same type of loading, are superimposed. If the shapes are similar, a shift of 20 % of rib length can be observed.

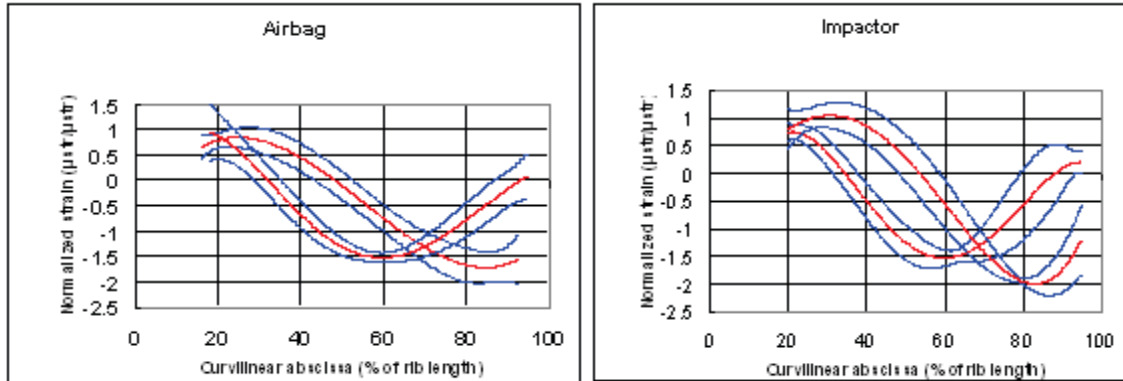


Figure 13: effect of angle on the strain profiles for airbag (left part) and impactor tests (right part)

### Effect of loading.

Figure 14 displays the comparison of the mean curves of strain profiles at 60 degrees and 90 degrees, respectively. The shapes of the strain profiles are similar for the two loadings, indicating that the rib fracture mechanism is the same for the two configurations.

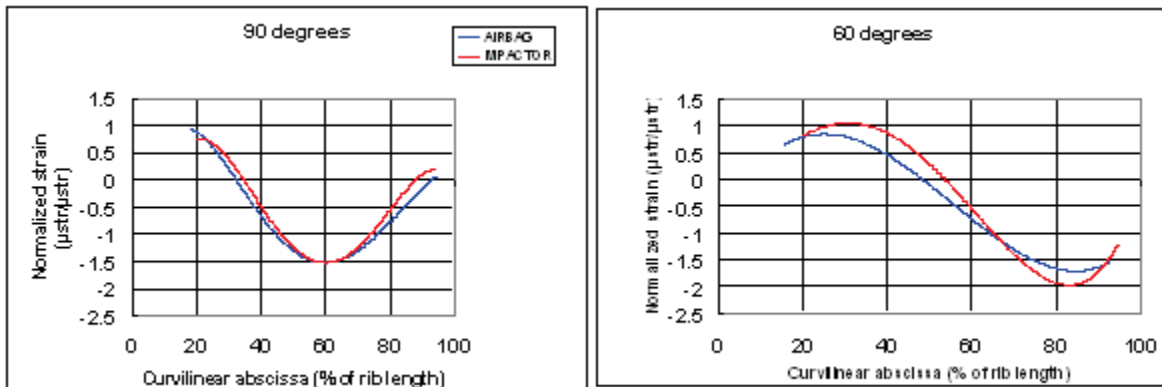


Figure 14: effect of loading on the strain profiles at 90 (left part) and 60 degrees (right part)

## **PERSPECTIVES**

The first perspective is to extend the analysis to the adjacent ribs, in order to see if the findings are identical. The second perspective regards the use of these data for the thorax validation of the Global Human Body Model. The authors think that the use of these data should be fruitful to validate the rib fracture mechanisms in various loadings and to understand how the soft and hard tissues interact. Then, the objectives will be to replicate these configurations with the finite-element model of the thorax, to validate the location of rib fractures and strain profiles. The results will be disseminated through the Center Of Expertise for the Thorax, which is the University of Virginia.

## **CONCLUSIONS**

In this paper, the results of twenty-four PMHS tests onto the thorax have been presented, with a focus on the strain profiles of the 5<sup>th</sup> rib on the impact side. Eight tests coming from the THOMO project have been added to existing tests published in a recent past, performed with the same methodology. The gathering of these two databases has allowed to build strain profile corridors in side and oblique impacts, with two different loadings, id est rigid impact and unfolded airbag impact.

The test results show that the rib fractures, which are the most frequent thorax injuries, appear in locations which depend on the loading direction.

The analysis of strain signals show that typical profiles can be established, whose shape depends on the loading direction. The location of minimum strain corresponds to the location of the rib fracture. This finding reinforce the conclusions of Trosseille et al (2008).

Corridors have been defined for four configurations, including two directions of forces and two types of loading applied to the thorax.

These strain profile corridors can be used for the validation of rib fracture mechanisms on human body models.

## **ACKNOWLEDGEMENTS**

The authors would like to thank the employees from CEESAR for their assistance: David Loury, Denis Dubois, Frédéric Loiseleux, Catherine Potier and Pascal Potier. They would like also to acknowledge those who have participated in the study: Erwan Lecuyer from LAB PSA-Peugeot-Citroën Renault SA.

This study is a part of of the THOMO project co-funded by the European Community FPth. The authors would like to gratefully thank the European Community and the different partners involved in this project ([www.thomo.eu](http://www.thomo.eu)).

The authors gratefully acknowledge the support of the University of Virginia and the Global Human Body Model Consortium.

This work could not have been done without the generous gift of body donors, through the center of the Body Donation to Science of the University René Descartes in ParisVth. A special thought to all of them.

## REFERENCES

- CHARPAIL, E., TROSSEILLE, X., PETIT, P., LAPORTE, S., LAVASTE, F., VALLANCIEN, G., Characterization of PMHS ribs: a new test methodology, Journal of Stapp Car Crash Conference, SAE Paper No 2005-22-0009, pp. 183-198.
- KEMPER A. R., MCNALLY C. , KENNEDY E. A., MANOOGIAN S. J., RATH A. L., NG T.P., STITZEL J.D., SMITH E.P., DUMA S.M., MATSUOKA F.. Material Properties of Human Rib Cortical Bone from Dynamic Tension Coupon Testing. Journal of Stapp Car Crash Conference, SAE Paper No 2005-22-0010, pp 199-230.
- KENT R., LESSLEY D., SHERWOOD C. . Thoracic Response to Dynamic, Non-Impact Loading from a Hub, Distributed Belt, Diagonal Belt, and Double Diagonal Belts. Journal of Stapp Car Crash Conference, SAE Paper No 2004-22-0022.
- KROELL, C.K., SCHNEIDER, D.C., NAHUM, A.M. Impact tolerance and response of the human thorax, Fifteenth Stapp Car Crash Conference, Paper No 710851.
- KROELL, C.K., SCHNEIDER, D.C., NAHUM, A.M., Impact tolerance and response of the human thorax II. Eighteenth Stapp Car Crash Conference Paper No 741187.
- LEBARBE M., POTIER P., BAUDRIT P., VALLANCIEN G. Thoracic Injury Investigation using PMHS in Frontal Airbag Out-of-Position Situations. Journal of Stapp Car Crash Conference, SAE Paper No 2005-22-0015, pp 323-342.
- POTIER P. Contribution méthodologique à la Thanatomécanique et à la Thanatométrie. Thesis, 2010.
- PETIT P., TROSSEILLE X., BAUDRIT P., GOPAL M. Finite Element Simulation Study of a Frontal Driver Airbag Deployment for Out-of-Position Situations. Journal of Stapp Car Crash Conference, SAE Paper No 2003-22-0011, pp 211-241.
- SHAW J., HERRIOTT R.G., MCFADDEN J.D., DONNELLY B.R., BOLTE J.H. (2006). Oblique and Lateral Impact Response of the PMHS Thorax. Journal of Stapp Car Crash Conference, SAE Paper No 2006-22-0007, pp147-167.
- SONG E., TROSSEILLE X., BAUDRIT P., Evaluation of Thoracic Deflection as an Injury Criterion for Side Impact Using a Finite Elements Thorax Model. Journal of Stapp Car Crash Conference, SAE Paper No 2009-22-0006, pp 155-191.
- TROSSEILLE, X., BAUDRIT P., LEPORT T., VALLANCIEN G. (2008). Rib Cage Strain Pattern as a Function of Chest Loading Configuration. Journal of Stapp Car Crash Conference, SAE Paper No 2008-22-0009, pp 205-231.
- TROSSEILLE, X., BAUDRIT P., LEPORT T., POTIER P., VALLANCIEN G. (2009). The Effect of Angle on the Chest Injury Outcome in Side Loading. Journal of Stapp Car Crash Conference, SAE Paper No 2009-22-0014, pp 403-419.
- VIANO D. C. Biomechanical Responses and Injuries in Blunt Lateral Impact. Thirty-third Stapp Car Crash Conference, Paper No 892432, pp 113-142.